

PNNL-28940

# **The neutronic impact of a variable-diameter Li-6 linear load on fuel-lattice power distributions and TPBAR rodworth**

National Security Internship Program

July 2019

Jonathan Crozier

## DISCLAIMER

This report was prepared as an account of work sponsored by an agency of the United States Government. Neither the United States Government nor any agency thereof, nor Battelle Memorial Institute, nor any of their employees, makes **any warranty, express or implied, or assumes any legal liability or responsibility for the accuracy, completeness, or usefulness of any information, apparatus, product, or process disclosed, or represents that its use would not infringe privately owned rights.** Reference herein to any specific commercial product, process, or service by trade name, trademark, manufacturer, or otherwise does not necessarily constitute or imply its endorsement, recommendation, or favoring by the United States Government or any agency thereof, or Battelle Memorial Institute. The views and opinions of authors expressed herein do not necessarily state or reflect those of the United States Government or any agency thereof.

PACIFIC NORTHWEST NATIONAL LABORATORY  
*operated by*  
BATTELLE  
*for the*  
UNITED STATES DEPARTMENT OF ENERGY  
*under Contract DE-AC05-76RL01830*

Printed in the United States of America

Available to DOE and DOE contractors from the  
Office of Scientific and Technical Information,  
P.O. Box 62, Oak Ridge, TN 37831-0062;  
ph: (865) 576-8401  
fax: (865) 576-5728  
email: [reports@adonis.osti.gov](mailto:reports@adonis.osti.gov)

Available to the public from the National Technical Information Service  
5301 Shawnee Rd., Alexandria, VA 22312  
ph: (800) 553-NTIS (6847)  
email: [orders@ntis.gov](mailto:orders@ntis.gov) <<https://www.ntis.gov/about>>  
Online ordering: <http://www.ntis.gov>

# **The neutronic impact of a variable-diameter Li-6 linear load on fuel-lattice power distributions and TPBAR rodworth**

National Security Internship Program

July 2019

Jonathan Crozier

Prepared for  
the U.S. Department of Energy  
under Contract DE-AC05-76RL01830

Pacific Northwest National Laboratory  
Richland, Washington 99354

## Abstract

Tritium-producing burnable absorber rods (TPBARs) are designed to produce tritium when irradiated in a pressurized water reactor (PWR), within a commercial fuel assembly. Within a TPBAR, annular ceramic pellets consisting of Lithium Aluminate  $\text{LiAlO}_2$  contain a given linear loading of Li-6, which undergoes neutron capture thus producing Tritium. Obtaining the proper Li-6 loading currently requires blending of powder prior to pellet manufacturing, or volume reduction of a higher lithium loading pellet to that of the desired loading.

This study demonstrates the neutronic performance of both inner and outer volume-reduced Li-6 pellets as comparable to that of a standard dimension, non-milled pellet by modelling 8,250 distinct fuel assembly lattices with Studsvik's CASMO5. Conditions included are at reactor Hot Full Power (HFP), Hot Zero Power (HZP) and Cold Zero Power (CZP) for 4.80-8.0 U-235 w/o, 8-24 TPBARs, 0-200 IFBAs, and 29-50 mg/in Li-6.

Modeling these possible assembly designs results in a maximum TPBAR rod worth of 900 pcm. A maximum difference in rod worth of 127 pcm and a maximum pin power RMS difference of .0007 shows that volume reduction is a viable option for achieving desired lithium loading. Greatest rodworth and power differences occur between standard dimension non-milled and outer-volume-reduced Li-6 loading.

## Summary

Milling the radii of a TPBAR's Lithium Aluminate pellet to a desired linear load of Li-6 does not significantly change its impact on lattice k-infinities, rodworth, pin powers and tritium production compared to that of a lattice composed of standard pellet TPBARs.

The maximum TPBAR rodworth is 900 pcm, and the highest absolute delta in rodworth is 127 pcm for which the standard pellet has a greater impact on the lattice eigenvalue than the outer-milled pellet. The maximum normalized pin-power is 1.200 and the greatest difference in RMS is .0007. The inner-milled pellet produces 2.504% more tritium at 25 GWd/MTU than the standard pellet when modeled as a lattice with reflective boundary conditions.

Future work includes incorporation of milled pellet lattices and cross sections into full core simulations for Watts Bar Unit 1 Cycles.

## Acronyms and Abbreviations

BP9	Burnable Poison 9
BP10	Burnable Poison 10
CASMO5	Method of Characteristics Lattice Physics Code
CZP	Cold Zero Power
EOC	End of Cycle
GWd/MTU	Gigawatt day per Metric Ton of Uranium
HFP	Hot Full Power
HZP	Hot Zero Power
IFBA	Integral Fuel Burnable Absorber
WABA	Wet Annular Burnable Absorber
comp	standard pellet
inner	inner-radii milled pellet
k-inf	characteristic eigenvalue
outer	outer-Radii Milled Pellet
pcm	percent-milli
RCCA	rod cluster control assembly

# Contents

Abstract.....	1
Summary .....	2
Acronyms and Abbreviations.....	3
Contents .....	4
1.0 Introduction and Motivation.....	6
2.0 Codes Used.....	7
3.0 Summary of Results .....	8
4.0 Methodology and Model Description.....	9
5.0 Results .....	14
5.1 Lattice 2-Group Rodworth at HFP, HZP, CZP .....	14
5.2 Lattice 2-Group Rodworth Deltas at HFP, HZP, CZP .....	15
5.3 Pin Power Maxima, Delta Distributions at HFP, HZP, CZP .....	16
5.4 Pin Power Delta Distributions at HFP, HZP, CZP .....	21
5.5 Lattice 2-Group Li-6 Burnup and Deltas .....	26
5.6 Lattice 2-Group Tritium Production .....	28
5.7 Lattice 2-Group Tritium Delta .....	29
5.8 CASMO5 Burnable Poison Modelling Decisions and Effects.....	30
6.0 Conclusions.....	31
7.0 References.....	32

## Figures

Figure 1.	Isometric cross-section of TPBAR materials and function specifications.....	10
Figure 2.	17x17 Assembly Lattice Fuel and Thimble Layout.....	11
Figure 3.	Burnable Absorber Locations for 1/8 Lattice Symmetry.....	12
Figure 4.	Full-symmetry CASMO5 input example for 0 IFBA, 24 TPBAR.....	13
Figure 5.	Lattice 2-Group TPBAR loading worth curves and TPBAR worth maxima....	14
Figure 6.	Lattice 2-Group TPBAR lithium loading worth differences.....	15
Figure 7.	Lattice 2-Group TPBAR k-inf comparisons and worth plot.....	16
Figure 8.	Lattice 2-Group TPBAR Base Pin Power Maxim.....	17
Figure 9.	Lattice 2-Group TPBAR Branch Pin Power Maxima.....	18
Figure 10.	Lattice 2-Group TPBAR Branch-Base Pin Power.....	19
Figure 11.	Lattice 2-Group TPBAR k-inf comparison and worth plot.....	20
Figure 12.	Normalized Base Pin Power Absolute Deltas.....	21
Figure 13.	Normalized Pin Power Absolute Delta Value.....	22
Figure 14.	HFP Normalized Pin Power Absolute Deltas at EOC.....	23
Figure 15.	HZP Branch and Base Loading Normalized Pin Differences.....	24
Figure 16.	CZP Branch and Base Loading Normalized Pin differences.....	25
Figure 17.	TPBAR Burnup Percent of Exposure for Lithium Loads.....	26
Figure 18.	TPBAR Burnup Percent of Exposure for Lithium Loads.....	27
Figure 19.	TPBAR Tritium Production across Lithium Loads.....	28
Figure 20.	TPBAR Tritium Production Deltas across Lithium Loads.....	29
Figure 21.	TPABR 'BP' Specifier and Smearing Effect on Burnup Percent.....	30

## Tables

Table 1.	Codes and Versions Used.....	1
Table 2:	Figure 5 Lattice Specifications.....	14
Table 3:	Figure 6 Lattice Specifications.....	15
Table 4:	Figures 7-11 Lattice Specifications.....	16
Table 5:	Figures 12-16 Lattice Specifications.....	21
Table 6:	Figures 17-18 Lattice Specifications.....	26
Table 7:	Figure 19 Lattice Specifications.....	28
Table 8:	Figure 20 Lattice Specifications.....	29
Table 9:	Figure 21 Lattice Specifications.....	30



## 1.0 Introduction and Motivation

The pressurized water reactor (PWR) employs the use of both soluble boron and burnable absorber rods to extend cycle length and to control reactivity. The use of IFBA, WABA and TPBAR burnable absorbers in core design reduce required soluble boron concentration in the reactor. Loaded into a 17x17 fuel assembly lattice guide tubes, TPBAR pin materials possess a high neutron absorption cross section which then produce isotopes, such as tritium, during the operating fuel cycle.

Tritium Producing Burnable Absorber Rods (TPBARs) are used by the National Nuclear Security Administration (NNSA) Tritium Readiness Program to irradiate a population of Lithium Aluminate targets in TVA Watts Bar cores. With a high peaking absorption cross section in the fast energy region, the Li-6 content undergoes neutron capture and produces Tritium. With two neutrons, this hydrogen isotope is relatively unstable and undergoes beta decay with a half-life of 12.32 years. This, in turn, requires replenishing of the decayed tritium in NNSA-managed stockpiles. Commercial and scientific tritium can also be used as a tracer in biomedical research, and is a viable source of fuel for fusion reactors as the deuterium-tritium reaction is a plausible magnetically-confined energy production mechanism.

The lithium content in Lithium Aluminate is primarily composed of Lithium-7 at 92.41% natural abundance, with the rest being Li-6. Tritium production primarily occurs in Li-6, making it necessary to increase the abundance of Li-6 in the TPBAR to achieve optimal core design. This results in a linear mass loading of Li-6 for the ceramic, sintered and annular pellets.

While a pellet volume reduction may effect ray-tracing results and Dancoff Factors, the neutron shadowing effects are accounted for in CASMO5. This study serves to demonstrate the minimal neutronic difference that exists between a current pellet and a volume reduction of a stock, higher-loaded pellet by analyzing TPBAR rodworth and pin power deltas. These results will allow for more flexibility when manufacturing TPBARs to meet the core designers neutronic requirements.

## 2.0 Codes Used

The following scripts in Table 1 were used to generate inputs, solve for lattice eigenvalues and pin-powers, and process results.

Table 1. Codes and Versions Used.

Codes	Version	Comments
Python	3.7.4	Used to write input deck and post-process CAS5 output
Studsvik's CASMO5	3.00.00	Method of Characteristics Eigenvalue Solver
Studsvik's CMSLink5	1.13.00	Cross section generating for Simulate5

### 3.0 Summary of Results

As the U-235 weight-percents increase from 4.80 w/o to 8.0 w/o: lithium burnup and tritium production decrease and Li-6 burnup distribution over exposure flattens, burnup deltas between loadings decrease, greatest BP9-BP10 differences shift towards EOC, TPBAR rodworths and deltas decrease, and pin power domains tighten.

As the lithium loadings increase from 29 mg/in to 50 mg/in: lithium burnup and tritium production decrease and Li-6 burnup distribution over exposure flattens, burnup deltas between loadings decrease and extrema shift towards EOC, greatest BP9-BP10 differences increase and shift towards EOC, TPBAR rodworths increase while deltas decrease, and pin power domains broaden while pin deltas between loadings decrease.

As the number of TPBAR increase from 8 pins to 24 pins: per-pin lithium burnup and tritium production marginally decrease, burnup deltas marginally increase towards EOC, BP9-BP10 differences decrease, TPBAR rodworths slightly decrease while deltas decrease, and pin power domains broaden significantly while pin deltas also increase significantly.

Across all dimensions, the following trends hold true: Li-6 burnup and tritium production over exposure is highest for inner-milled pellets, Li-6 burnup and tritium production difference is greatest between inner-milled and standard pellets, standard pellets have the highest rodworths over exposure (followed by inner-milled, then outer-milled pellets), rodworth difference is greatest between standard and outer-milled pellets, and pin power extrema is broader for the standard pellet than it is for the milled pellets, although the difference is greater with the outer-pellets than it is the with inner-pellets.

As such, the greatest TPBAR rodworth is at 900 pcm for a lattice with 4.80 w/o, 50 mg/in Li-6, 8 TPBAR and 0 IFBA. The same lattice at 29 mg/in has the greatest difference between loads with an absolute delta of 127 pcm between outer-milled and standard pellets. The greatest difference in RMS between radial pin power distributions is .0007. The results demonstrate that milled pellets of higher initial Li-6 linear loading perform comparably to standard pellets.

## 4.0 Methodology and Model Description

The methodology employed in this study consists of the construction of a case matrix that includes a wide range of possible fuel assembly lattice designs with a variable number of TPBARs, IFBAs and weight percent. This is to study the lattice global reactivity effects in eigenvalue and the lattice local effects to pin power distribution and TPBAR rodworth.

Lattices were constructed for linear mass loads of Li-6 from 29 mg/in to 50 mg/in, which accounts for a load domain broader than that in current use. Each given lattice geometry, weight percent specification, TPBAR and IFBA specification was modelled to a given linear TPBAR Li-6 mass loading by way of three distinct models: current pellet thickness, machining the inner radius and machining the outer radius. These cases were modelled in CASMO5 under three distinct reactor power conditions in order to neutronically differentiate between loading impacts across core operations.

The case matrix yielded 8,250 distinct CASMO5 runs across the domain of state-points between 0-80 GWd/MTU for 6 cases in each run, thus accounting for the eigenvalue impact of a pulled TPBAR at HFP, HZP, and CZP which results in the calculation of TPBAR rod worth. A normalized pin power distribution was also plotted for each state point exposure, as well as the Lithium-6 number density with CASMO5's Monte Carlo Punch card.

The scope of this study's case matrix is as follows:

- Enrichments: 4.80 - 8.0 w/o U-235
- IFBA: 0 - 200
- TPBAR: 8 - 24
- Lithium loadings [mg/in]: 29 - 50
- Lithium loading mechanisms: current pellet thickness, inner/outer radius reduction

The CASMO5 lattice physics code uses method of characteristics to model the single lattices effectively creating an infinite core with reflective boundary conditions on each side. The model does not account for spacer grids, intermediate flow mixers, and the impact of control rods since the goal of the study is to isolate the impact of lithium loading. The lattices also account for the middle of the active fuel region as this is where the TPBAR's impact on core power and neutron population is the greatest. As such, axial fuel blankets of lower enrichments and reflectors are not modelled. The central in-core detector is also not modelled. The fuel lattice structure, fuel pin, TPBAR, IFBA, and cladding material properties, dimensions and specifications are consistent with those used in TVA Watts Bar cycles.

The TPBAR was explicitly modelled following without smearing as follows (from outermost to inner material): Reactor Grade type 316 stainless steel cladding, nickel-plated Zircaloy-4 Tritium Getter, Lithium Aluminate Pellet, Zircaloy-4 Liner. The spacing between materials was backfilled with Helium, and the aluminide coating on the inner surface of the clad was not modelled since it is neutronically invisible. Pellet and pellet-column lengths are approximately 1" and 132", respectively, while the length of the stainless-steel cladding is 152" from tip to tip [1].

Figure 1 below depicts the cylindrical components of the TPBAR, with the annular Lithium Aluminate pellet enclosed by stainless steel cladding which encircles a metal getter tube. When tritium is produced from Li-6 neutron capture and fission, it chemically reacts and is captured by the getter as a hydride.

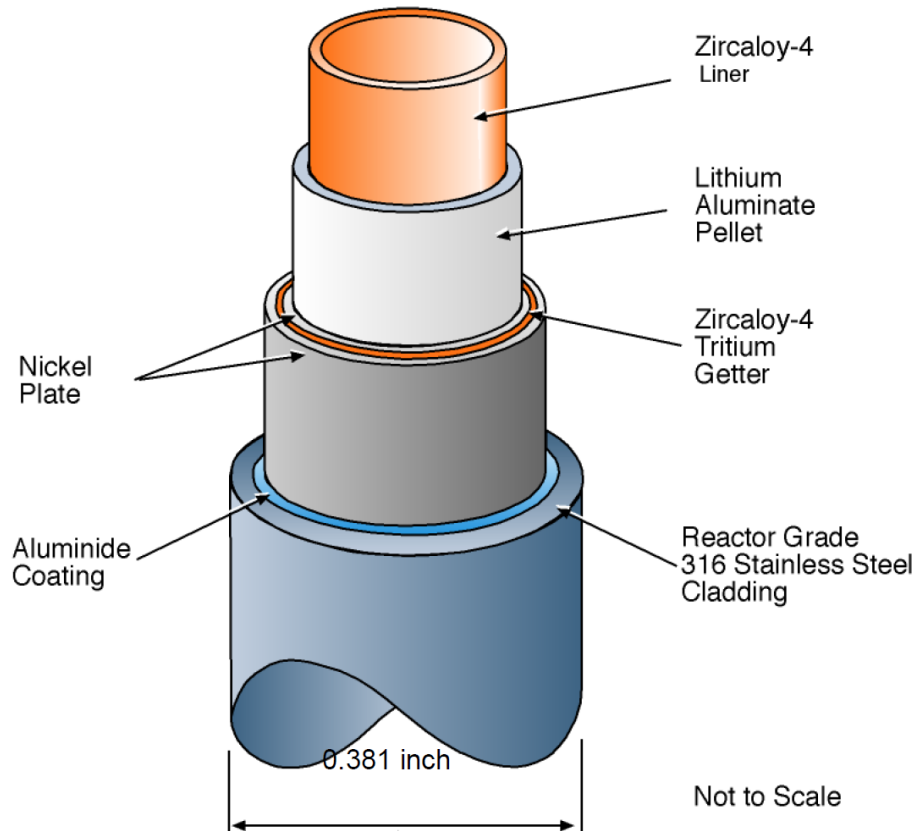


Figure 1: Isometric cross-section of TPBAR materials and function specifications (Ref. 1, Figure 1)

The following figure depicts the radial layout of guide tubes (GT) with respect to a central instrument tube (IT) and fuel pins in a 17x17 assembly lattice. Each lattice contains 24 GTs, or thimbles, into which rod cluster control assembly (RCCA) rodlets or burnable poison rods can be inserted. The central IT can house an in-core neutron detector. Each tube is Zircaloy-4. Small gaps exist in between lattices to allow for neutron moderation [2].

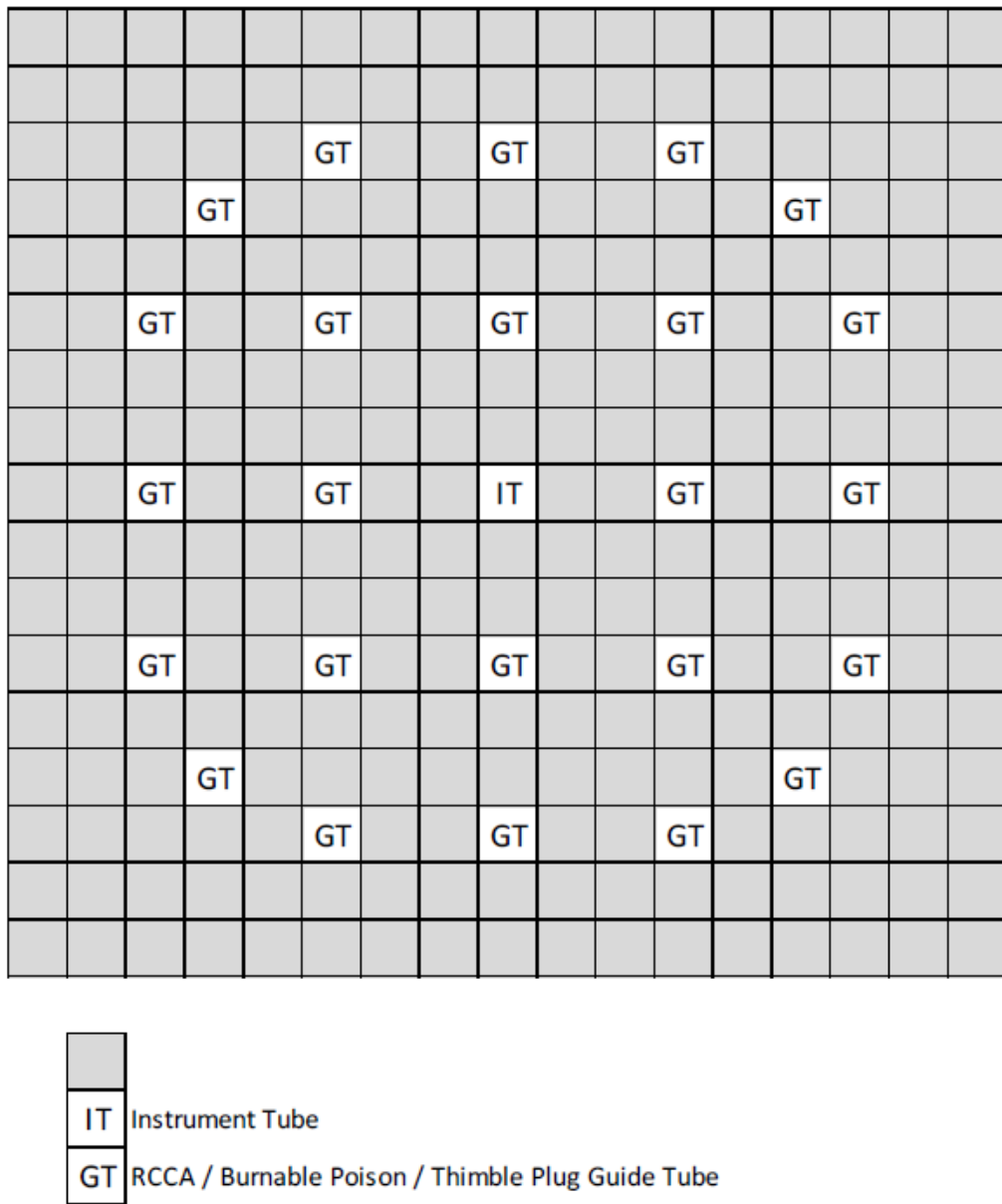


Figure 2: 17x17 Assembly Lattice Fuel and Thimble Layout (Ref. 2, Figure 3)

Figure 3 highlights the octant-symmetric input arrangements of burnable absorber rods which can house a WABA, or TPBAR in a blue-specified square. Note that IFBA can exist in any grey fuel rod-designated position.

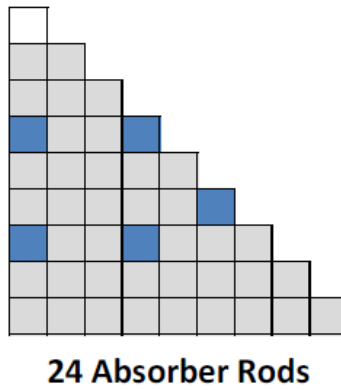


Figure 3: Burnable Absorbers for 1/8 Lattice Symmetry  
(Ref. 2, Figure 5)

The following full-symmetry map is a CASMO5 visual output of an assembly lattice which contains 24 TPBAR and no IFBA. Note that TPBAR are explicitly modelled and that the center in-core detector location is filled with moderator. Also note that the lower-right hand TPBAR is in fact defined as a removable rod in the CASMO5 input to allow for rodworth calculations.

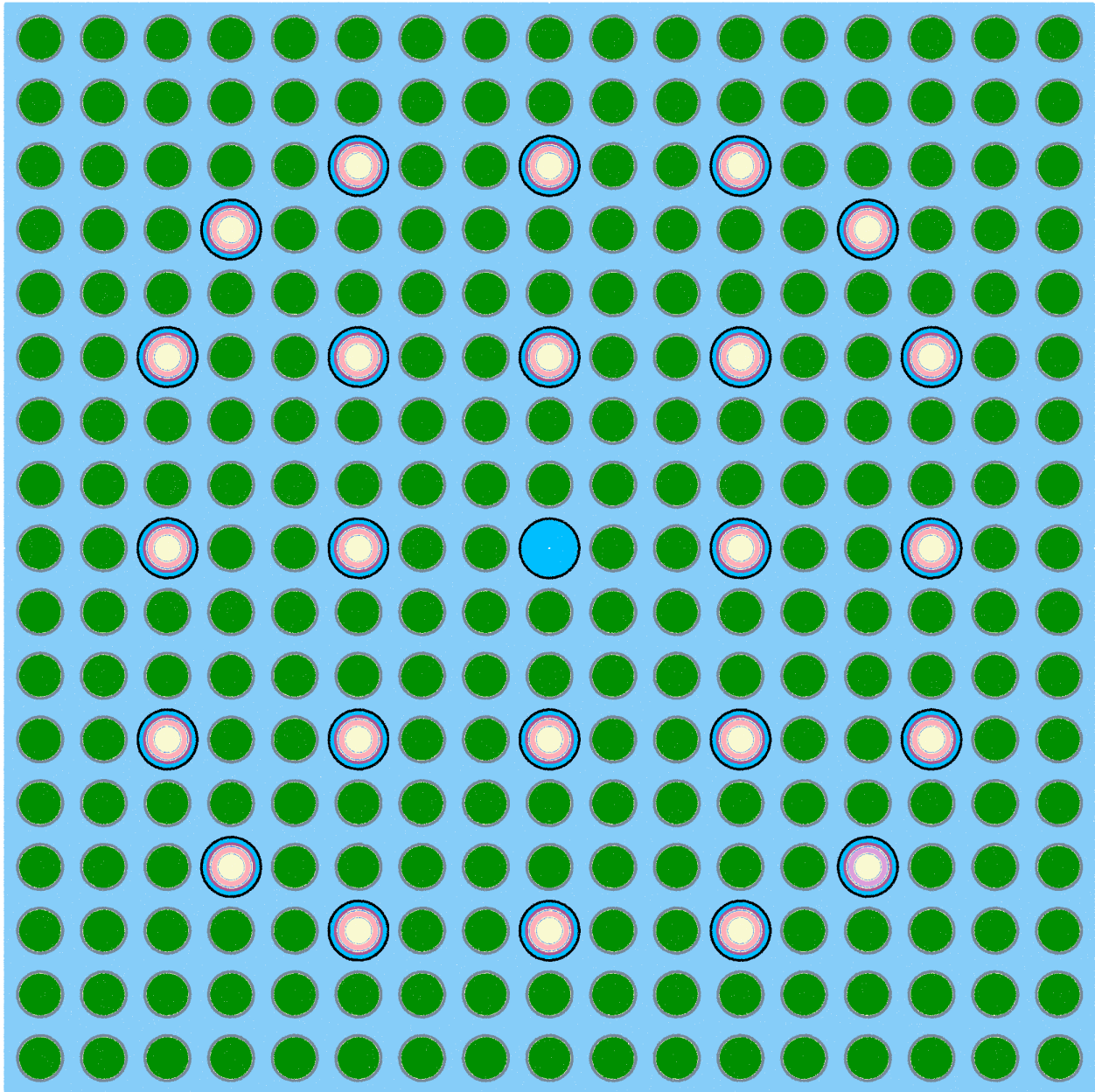


Figure 4: Full-symmetry CASMO5 input example for 0 IFBA, 24 TPBAR



## 5.0 Results

A rodworth maximum and delta between Li-6 loading of 900 pcm and 127 pcm, respectively, depict milled pellet neutronics as being strongly comparable to that of a standard pellet.

### 5.1 Lattice 2-Group Rodworth at HFP, HZP, CZP

The maximum TPBAR worth is 900 pcm for a regular lithium load at HFP, compared to an average rodworth of 622 pcm. The below Figure 5 depicts the rodworth curves versus statepoint exposure, followed by Table 2 which explicitly defines the lattice parameters of the respective worth maxima. The HZP and CZP max worth values are 811 pcm and 560 pcm, respectively.

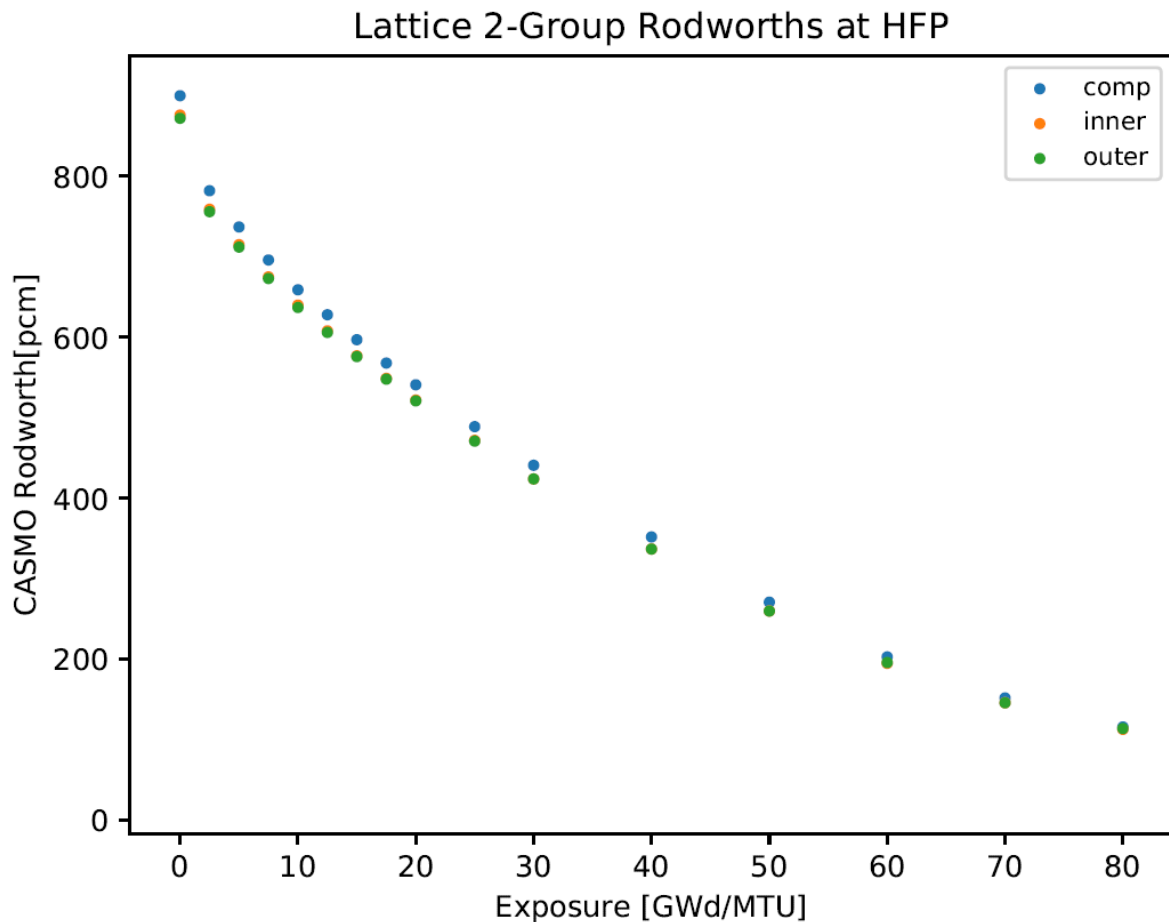


Figure 5: Lattice 2-Group TPBAR loading worth curves and TPBAR worth maxima

Table 2: Figure 5 Lattice Specifications

Rodworth Maxima [pcm]	900	Exposure [GWd/MTU]	0
U-235 Enrichment [w/o]	4.80	Number of TPBAR	8
Lithium Loading [mg/in]	50	Number of IFBA	0

## 5.2 Lattice 2-Group Rodworth Deltas at HFP, HZP, CZP

The maximum difference in TPBAR worths between lithium loading types is 127 pcm, for the same lattice as in Figure 5, with the exception of a lower lithium load of 29 mg/in. The average maximum TPBAR worth for the 4.80 w/o is 57 pcm. Figure 6 depicts the rodworth difference plots over exposure between the loading types.

Note that the inner loading difference is more significant than the outer loading difference. HZP and CZP max differences are 120 and 87 pcm, respectively, for the same lattice.

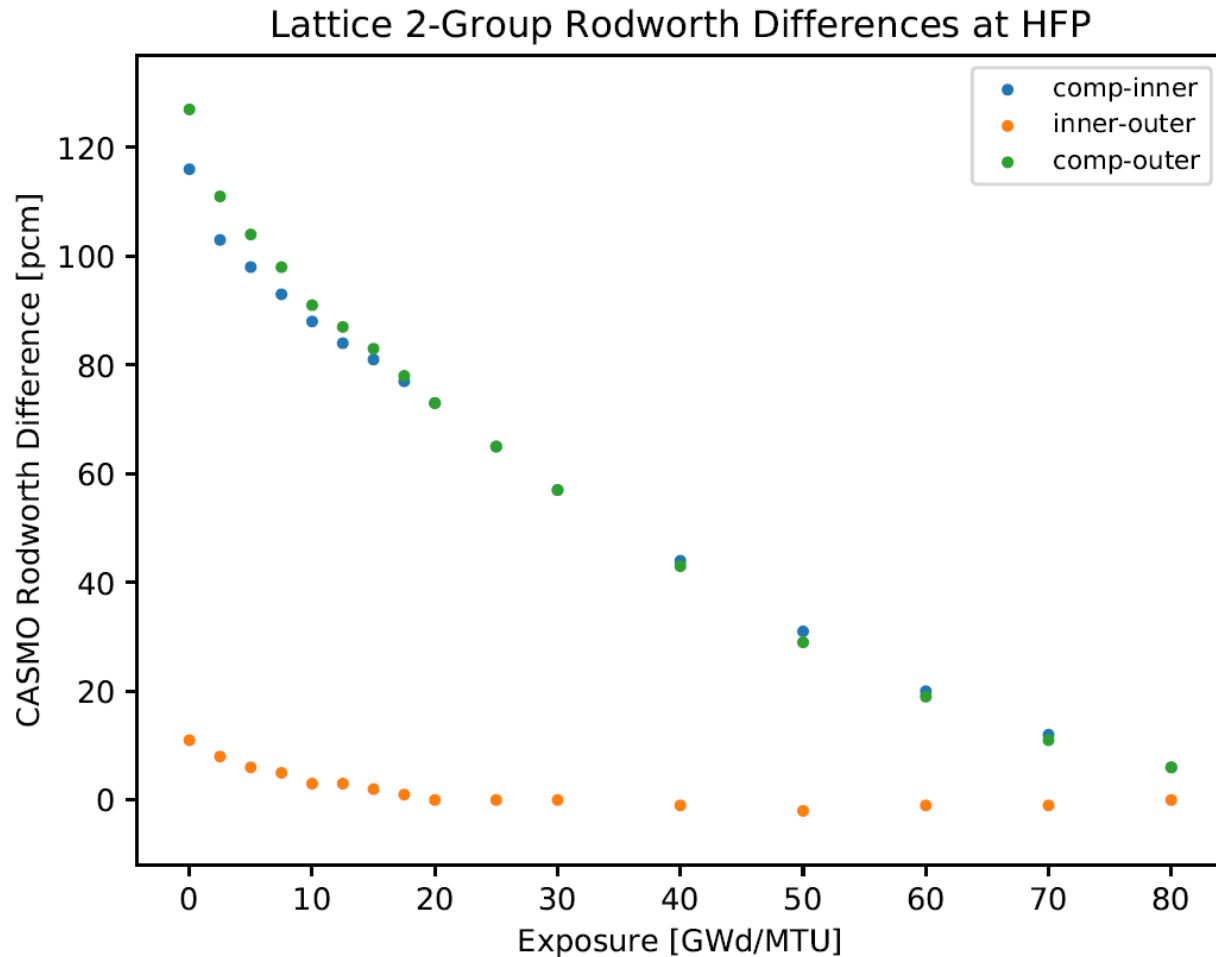


Figure 6: Lattice 2-Group TPBAR lithium loading worth differences

Table 3: Figure 6 Lattice Specifications

Rodworth Max Delta [pcm]	127	Exposure [GWd/MTU]	0
U-235 Enrichment [w/o]	4.80	Number of TPBAR	8
Lithium Loading [mg/in]	29	Number of IFBA	0

### 5.3 Pin Power Maxima, Delta Distributions at HFP, HZP, CZP

The following pin power extrema plot can be generated for identical lattices in order to further compare lithium loading effects. Inner and outer radii-varying lithium load trends in pin power extrema track comparably to the nominal pellet lithium loading. Note that the maximum occurs for the 'comp' loading case marginally above those of the inner and outer cases at HFP.

Note that Section 5.3's Figures correspond to the lattice specifications of Table 4.

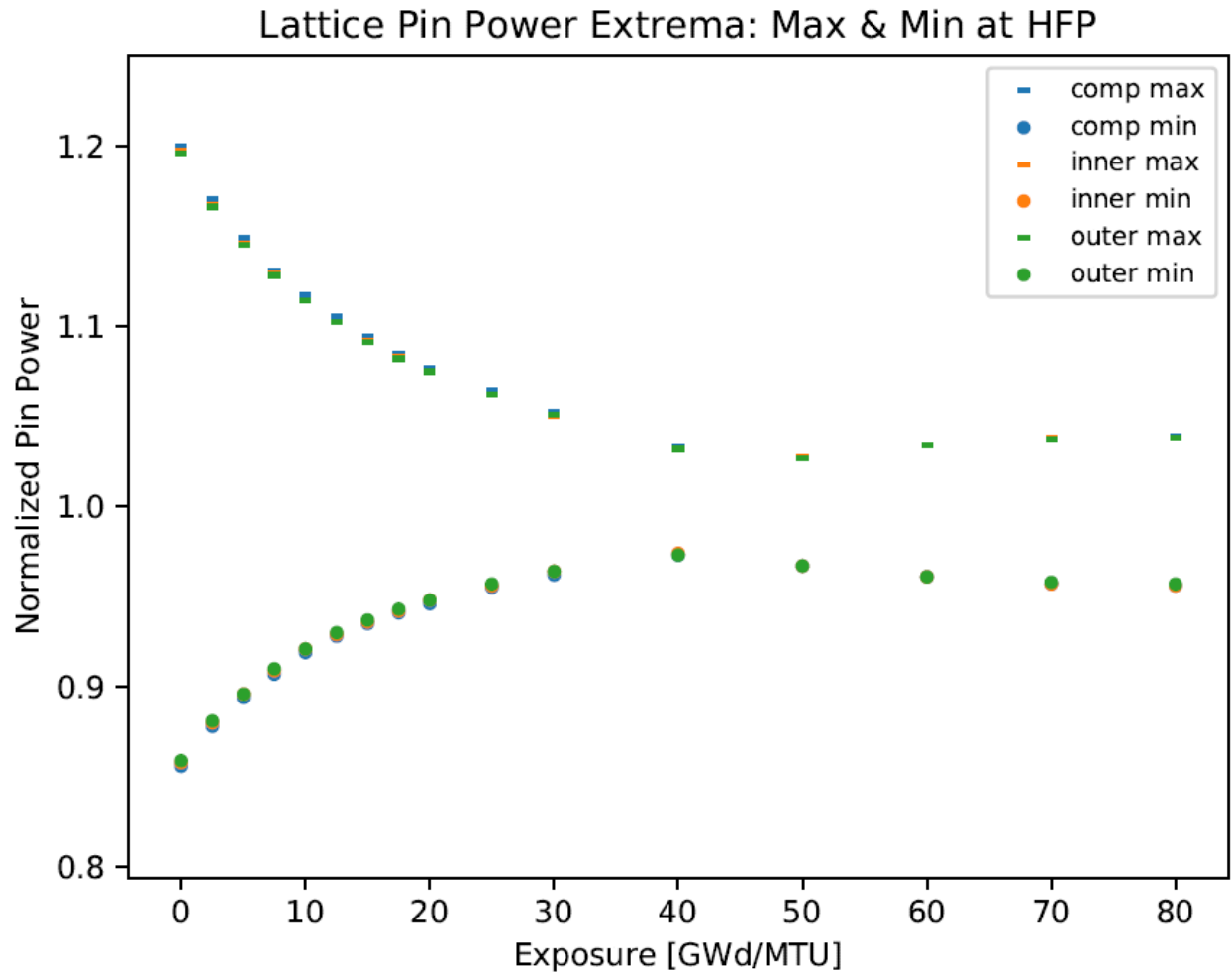


Figure 7: Lattice 2-Group TPBAR k-inf comparison and worth plot

Table 4: Figures 7-11 Lattice Specifications

Norm. Base Pin Max	1.200	Exposure [GWd/MTU]	0
U-235 Enrichment [w/o]	4.80	Number of TPBAR	24
Lithium Loading [mg/in]	50	Number of IFBA	128

The maximum normalized base pin power is 1.200, as per Figure 8, with a global average maximum of 1.1147 for the 4.80 w/o lattices. See the below figure for the pin power distribution for when no TPBAR's are withdrawn.

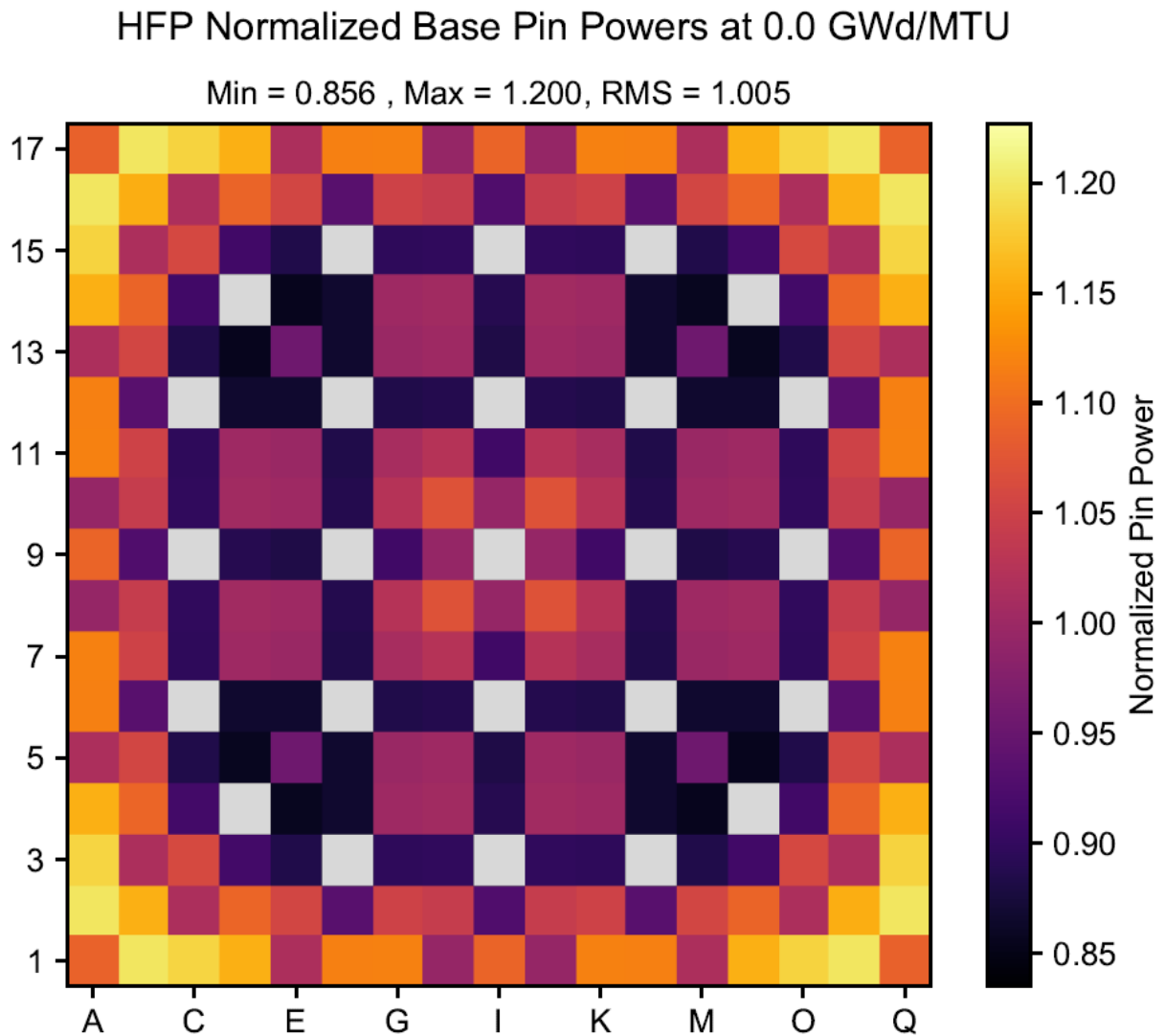


Figure 8: Lattice 2-Group TPBAR Base Pin Power Maxima

The below figure depicts the same lattice power distribution as defined in Table 4 at HFP, with the exception of a single pulled TPBAR in the lower right of the lattice. Notice the increase in max normalized pin power to 1.227.

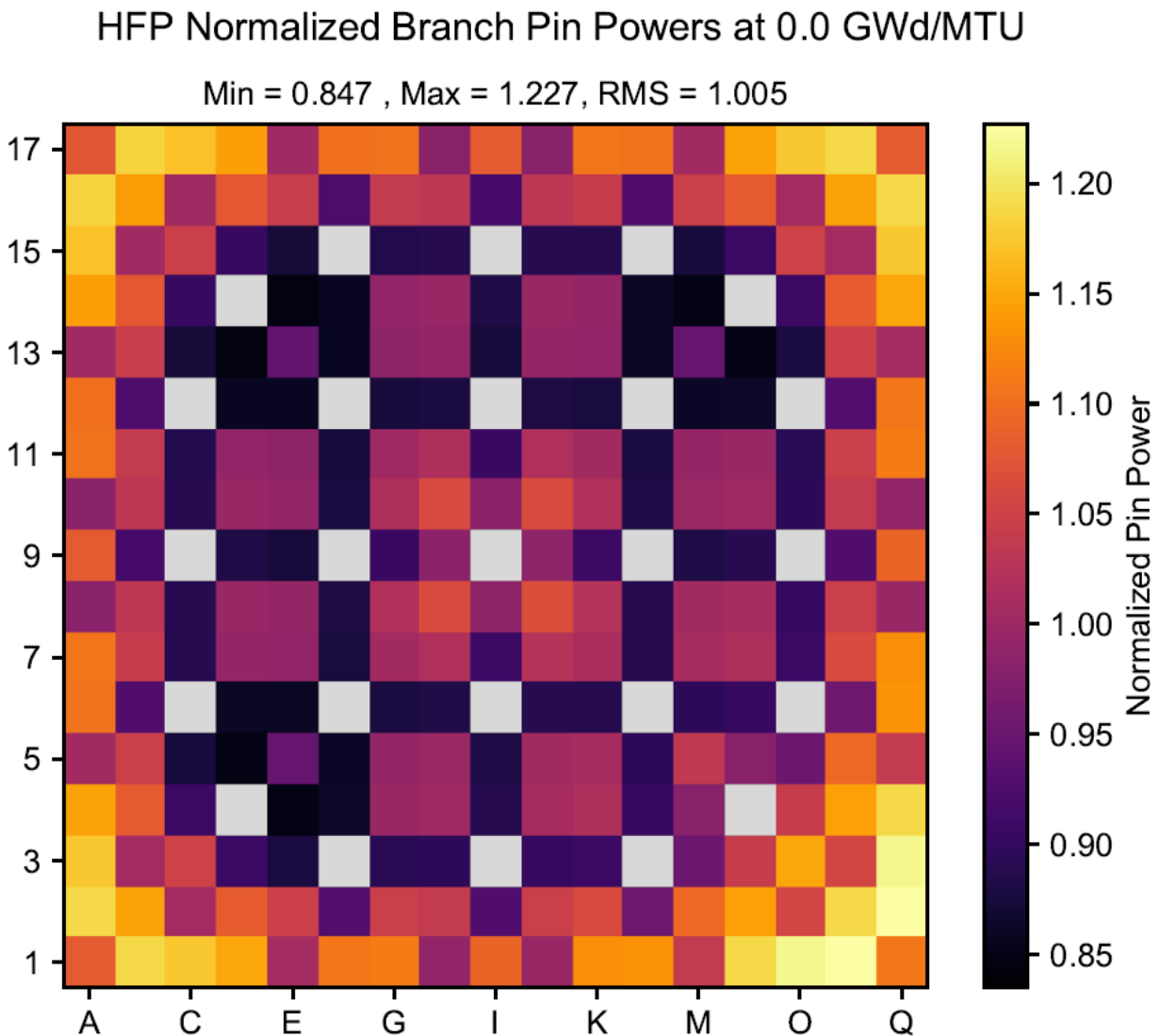


Figure 9: Lattice 2-Group TPBAR Branch Pin Power Maxima

The difference between the branch case (TPBAR pulled) and base case (TPBAR inserted) for the same lattice can be seen in the following Figure 10. Note the manner in which the highest degree of difference between the pin power maps appropriately congregate around the guide tube of the pulled TPBAR.

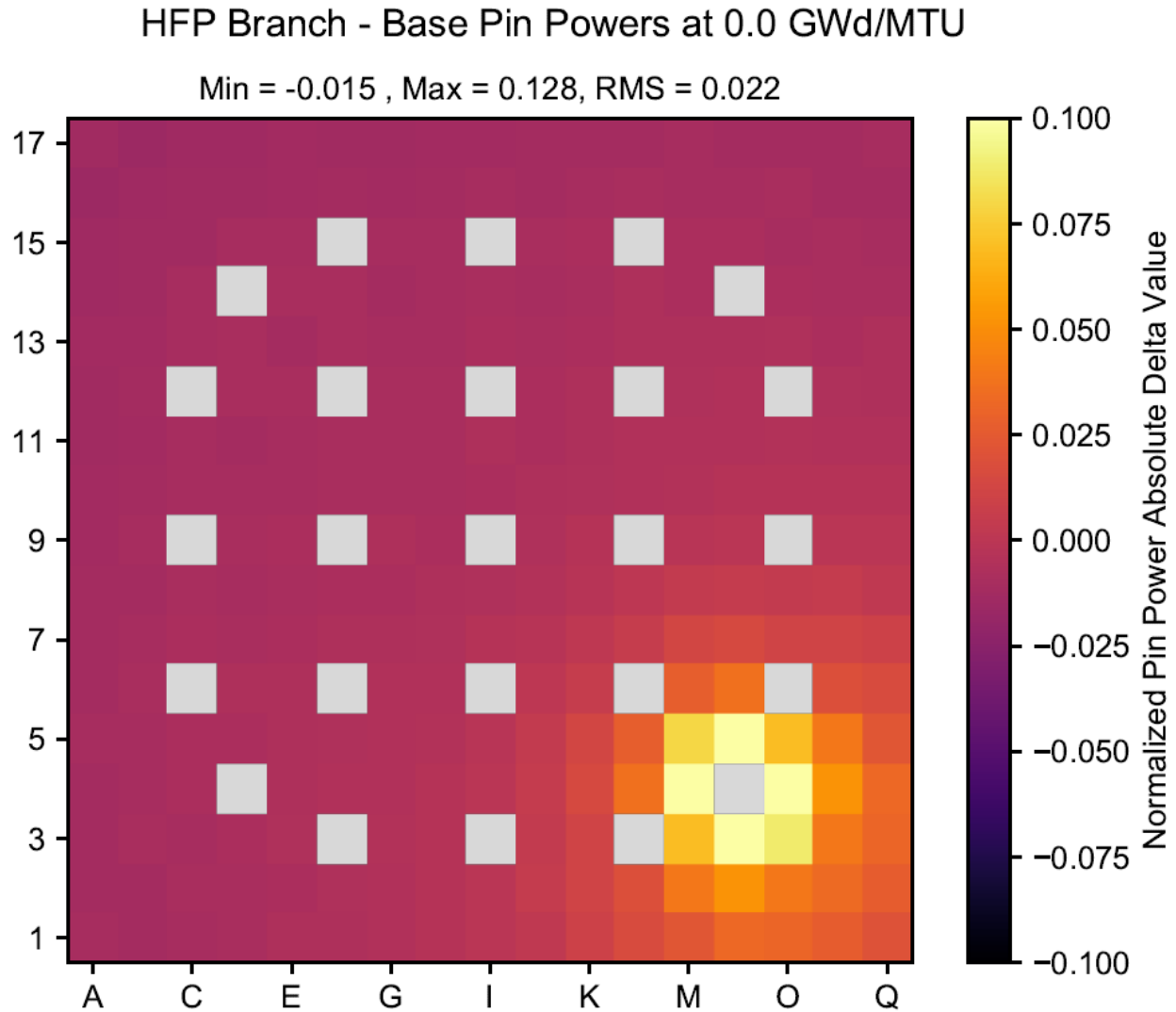


Figure 10: Lattice 2-Group TPBAR Branch-Base Pin Power

Note that that this difference in pin power can be directly related to a difference in lattice eigenvalue, which defines TPBAR rod worth at 500 pcm. Despite a peak pin power at 0 GWd/MTU, the point of greatest rodworth for this lattice is at 12 GWd/MTU, as per the following Figure 11.

The orange data point at 0 GWd/MTU corresponds to Figure 8's radial profile, the blue data point at 0 GWd/MTU corresponds to Figure 9's radial profile, and the green 'x'-specified data point at 0 GWD/MTU corresponds to Figure 10's radial profile.

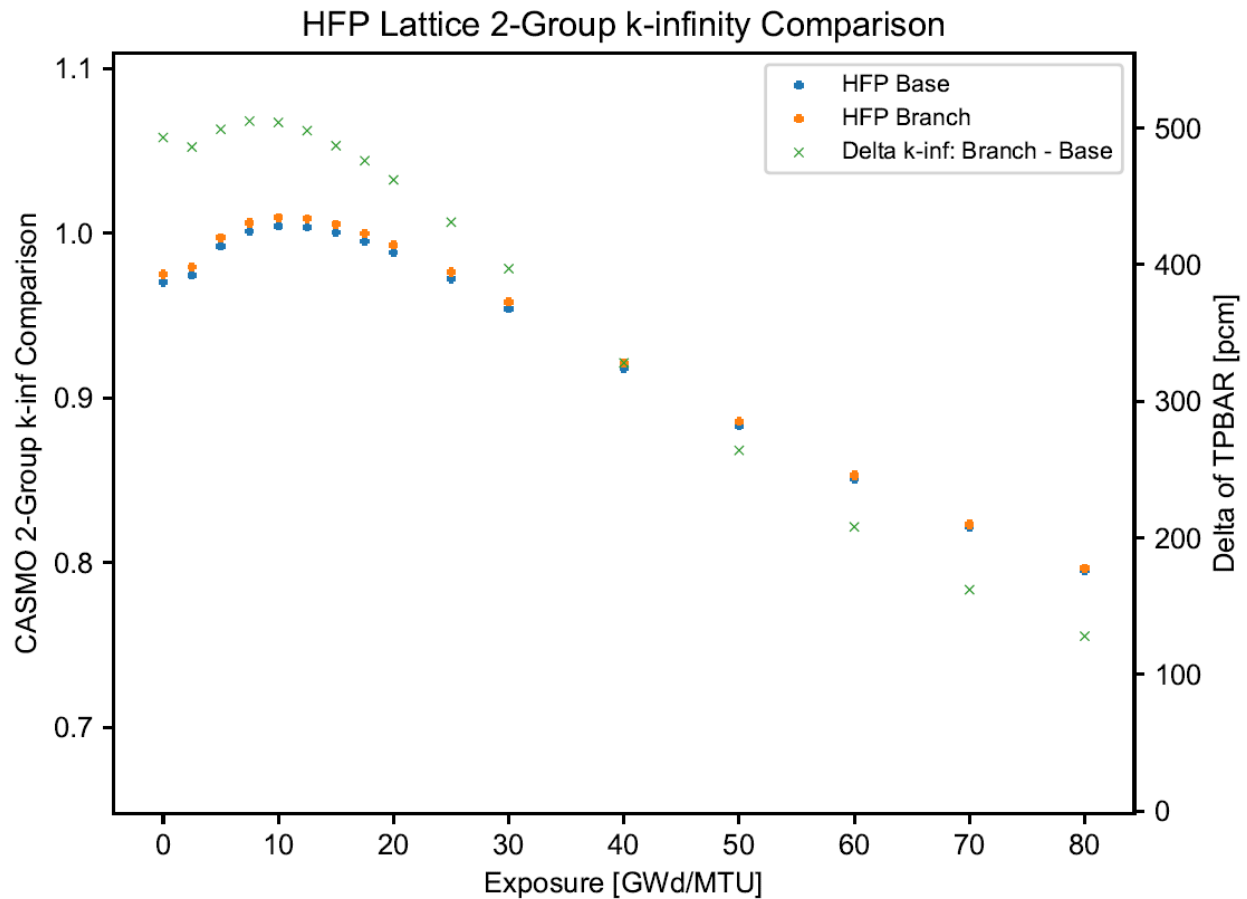


Figure 11: Lattice 2-Group TPBAR k-inf comparison and worth plot

## 5.4 Pin Power Delta Distributions at HFP, HZP, CZP

The following plots define the comparison of pin power distributions between loading types, and depict power distributions over exposure as nearly identical across lithium loads. The following Figure 12 shows the maximum difference in base pin powers, with Table 5 defining the lattice parameters. This lattice is indicative of the maximum differences between normalized pin power distributions. The following Figure 12, 13, 14 depict the maximum differences of the lattice at HFP, HZP and CZP, respectively for both branch and base cases.

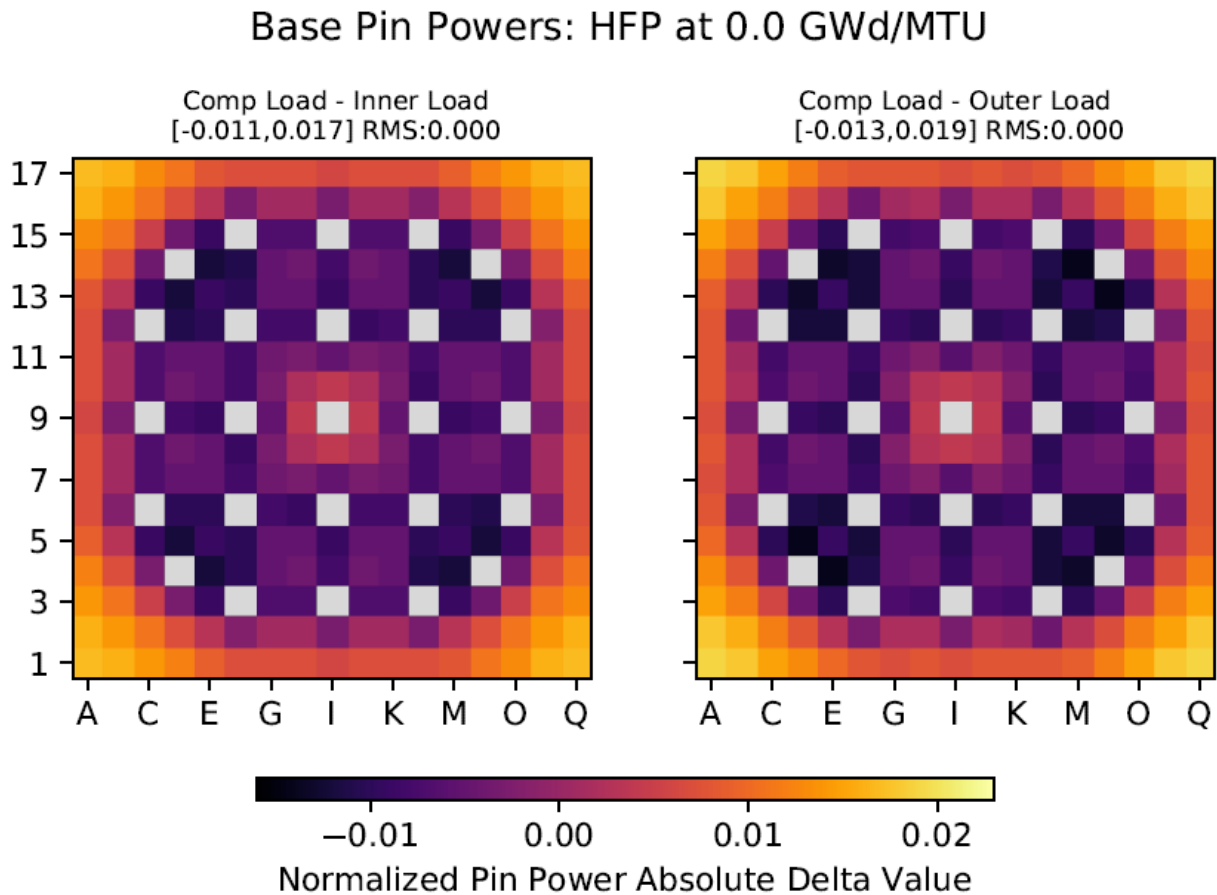


Figure 12: Normalized Base Pin Power Absolute Deltas

Table 5: Figures 12-16 Lattice Specifications

Max Norm. Pin Delta	.015 [comp-inner]	Exposure [GWd/MTU]	0
U-235 Enrichment [w/o]	4.80	Number of TPBAR	24
Lithium Loading [mg/in]	29	Number of IFBA	0



The following plot depicts the branch case pin power differences for the same lattice as defined in Table 13. These plots depict the maximum differences between loading types at HFP operating conditions.

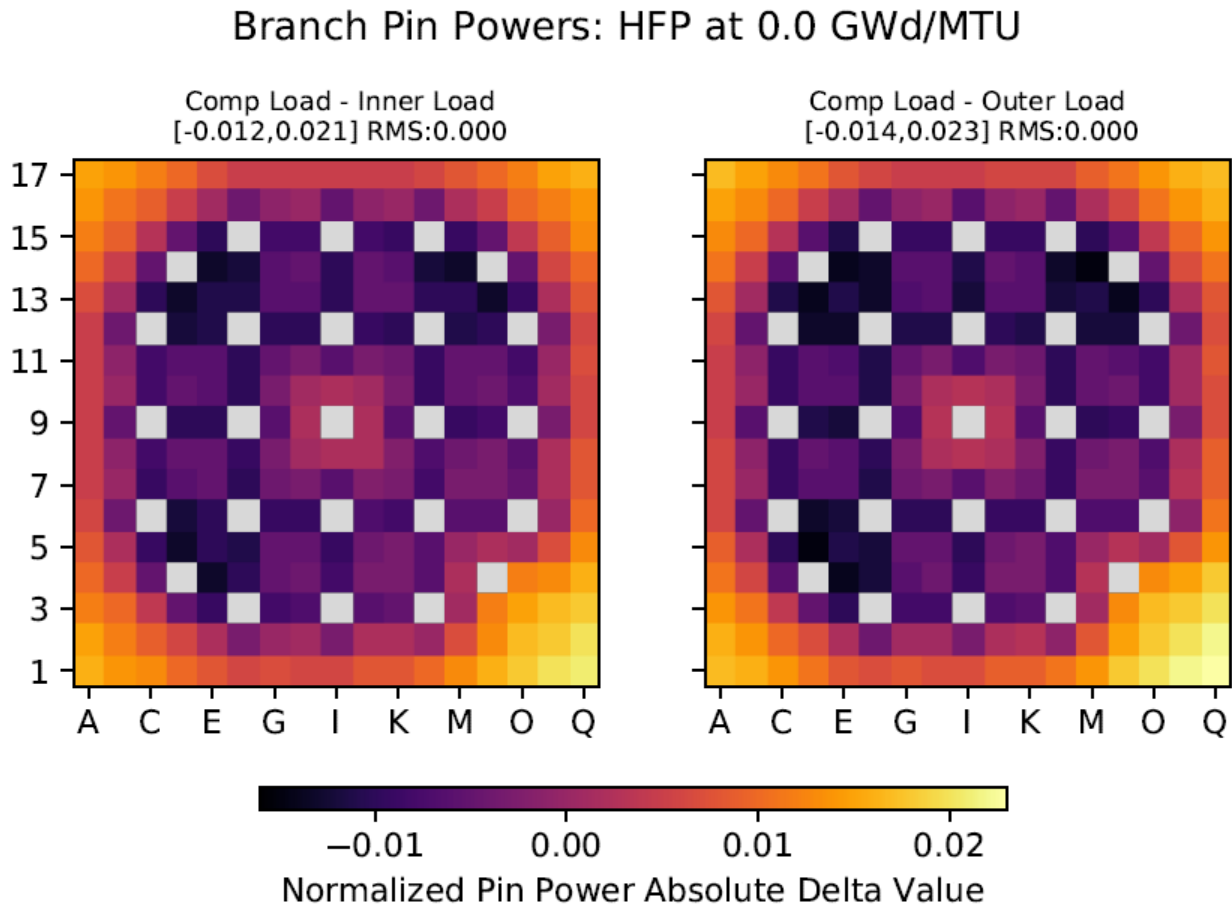


Figure 13: Normalized Branch Pin Power Absolute Deltas

It is also worth noting that over the course of the cycle, the difference shifts from the outer-edges of the lattice towards the center of the lattice in a more even distribution. Note the following plot of Table 5's base case HFP lattice at 80 GWd/MTU, which contains the most minimal differences overall. There are slightly higher absolute deltas further from the lattice boundary.

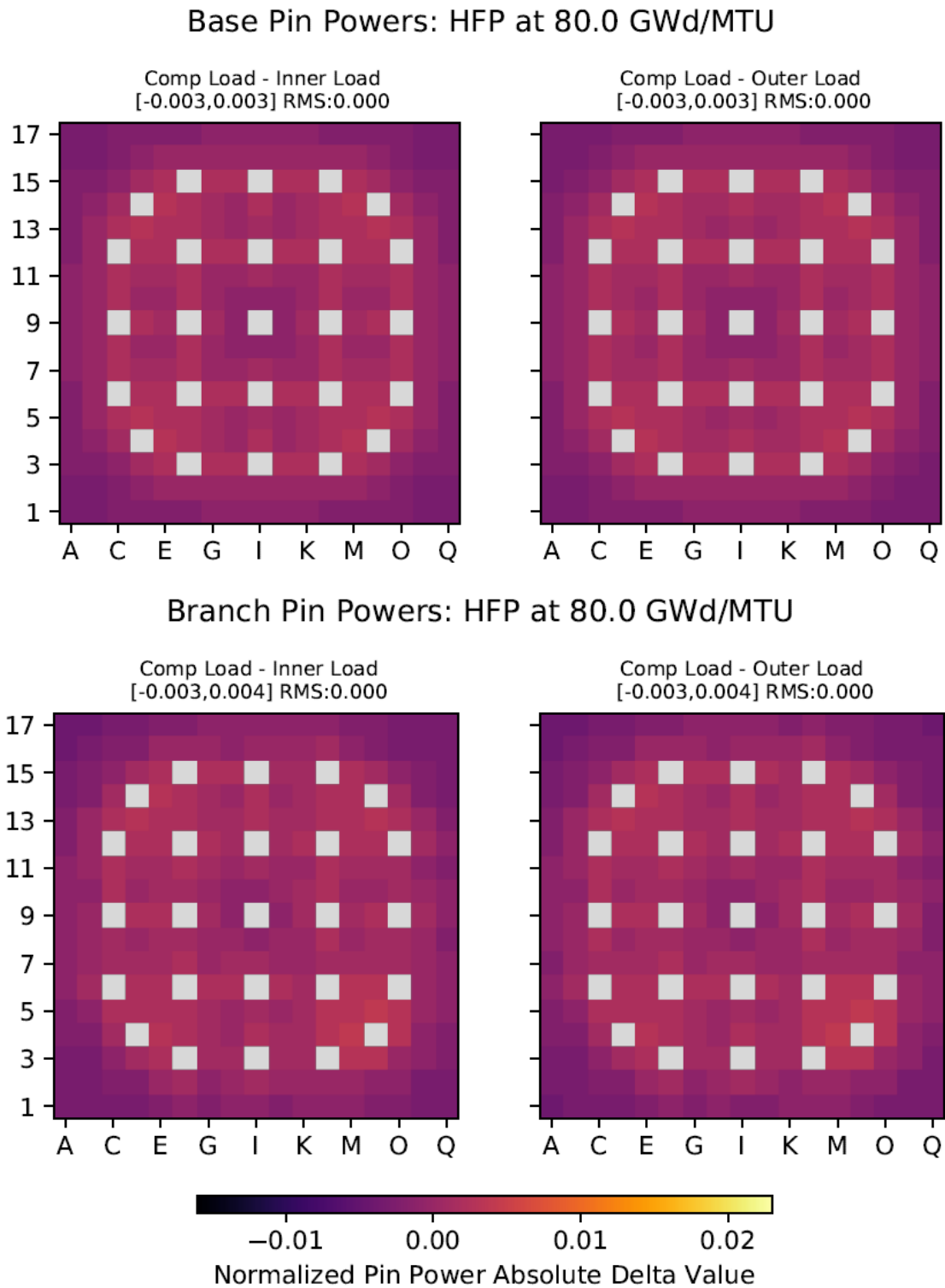


Figure 14: HFP Normalized Pin Power Absolute Deltas at EOC

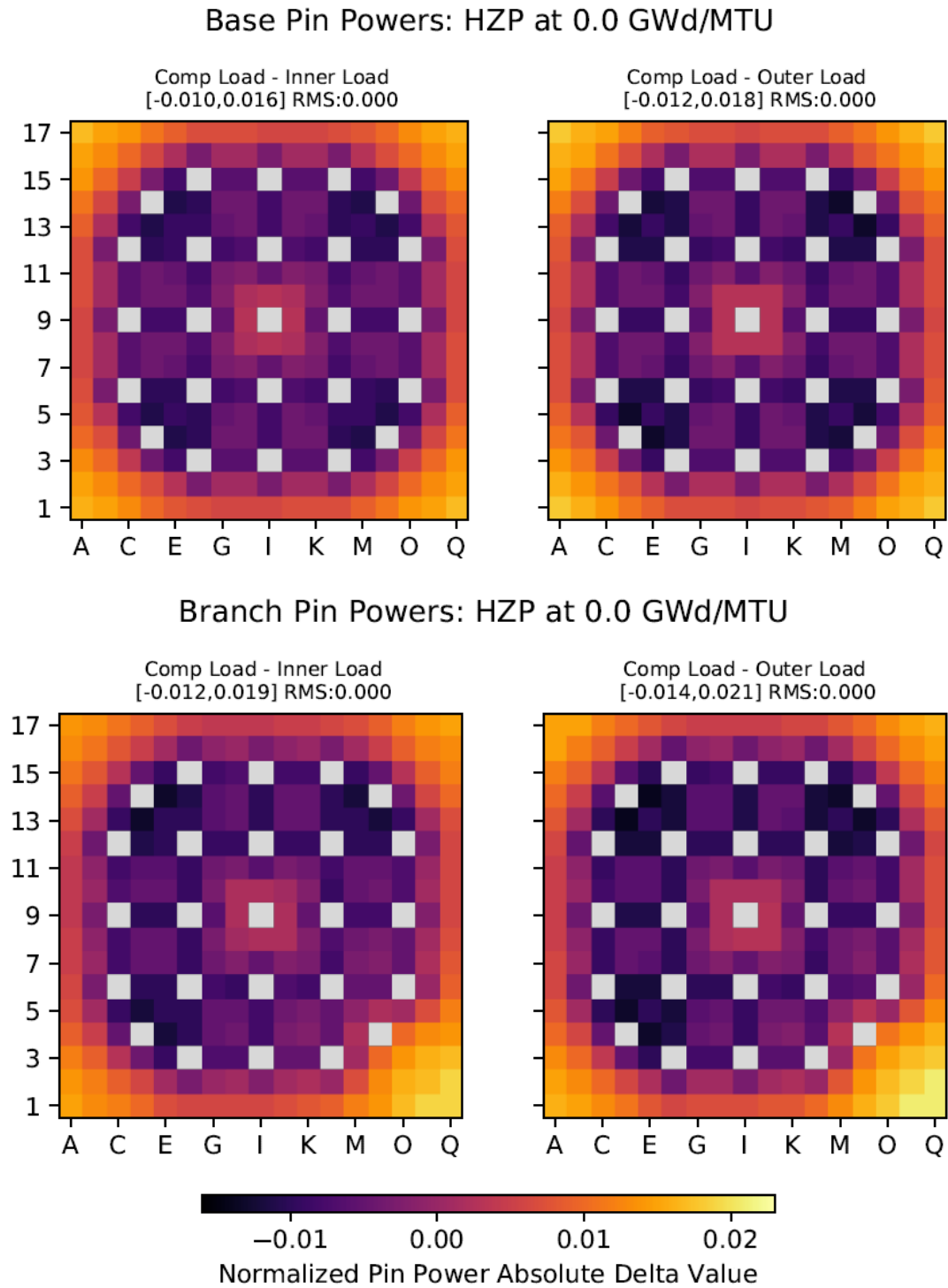


Figure 15: HZP Branch and Base Loading Normalized Pin Differences

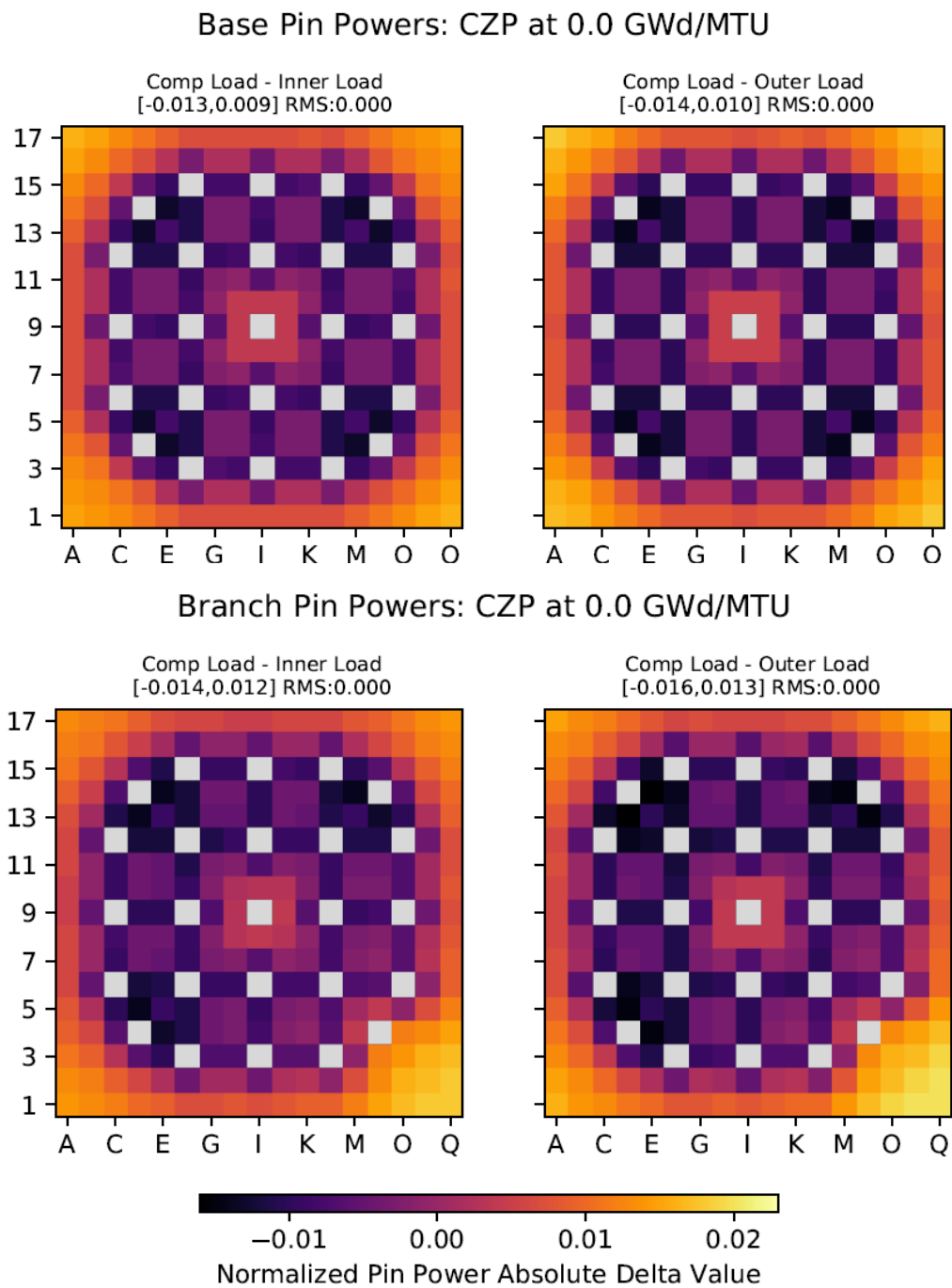


Figure 16: CZP Branch and Base Loading Normalized Pin Differences

## 5.5 Lattice 2-Group Li-6 Burnup and Deltas

Tritium production is a direct function of Li-6 burnup, which can be plotted as per isotopic abundances over the course of a cycle relative to initial Li-6 number density. Note that the Li-6 content is modelled as a non-removable burnable poison in CASMO5 as BP9. Below Figures illustrate burnup across lithium load. Note that maximum difference occur in the middle of the cycle, whereas minimal differences occur at beginning and end of cycle.

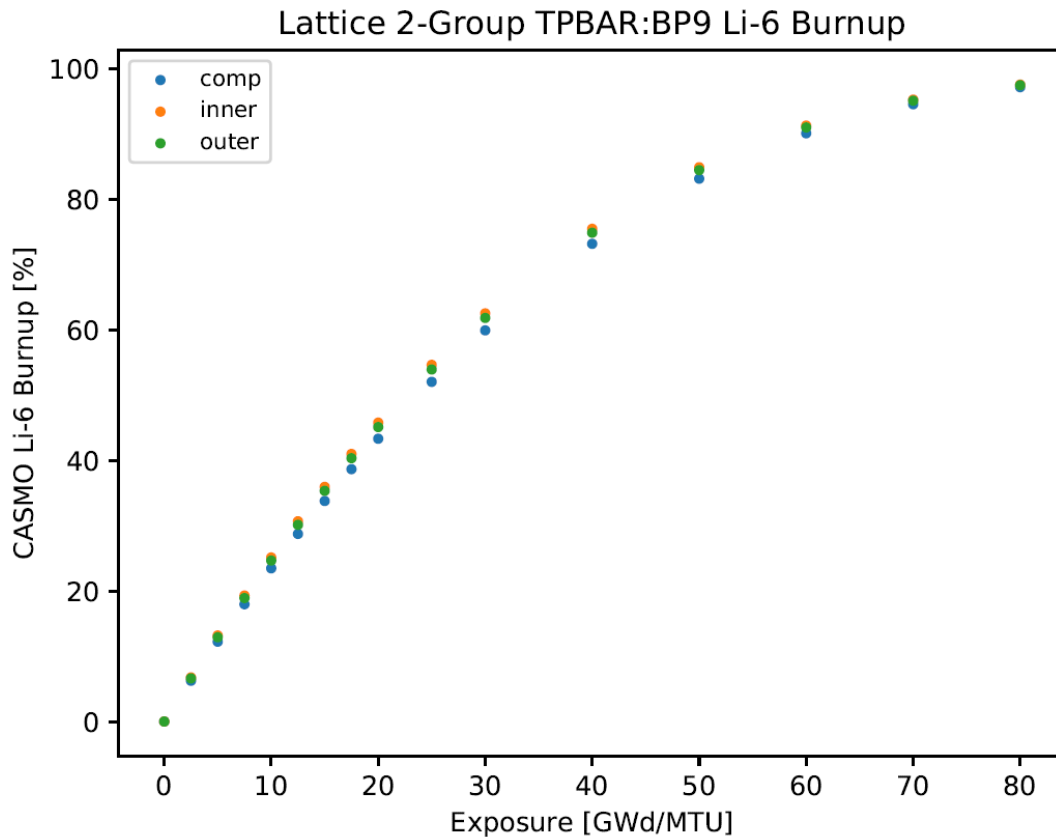


Figure 17: TPBAR Burnup Percent of Exposure for Lithium Loads

Table 6: Figures 17-18 Lattice Specifications

Maximum Burnup [%]	97.6240, inner	Exposure [GWd/MTU]	80
U-235 Enrichment [w/o]	4.80	Number of TPBAR	8
Lithium Loading [mg/in]	29	Number of IFBA	0

The greatest absolute difference in Li-6 burnup percent occurs at 25 GWd/MTU with an absolute difference of 2.504%, for the inner radii-varying load is significantly greater than that of the normal pellet load's burnup.

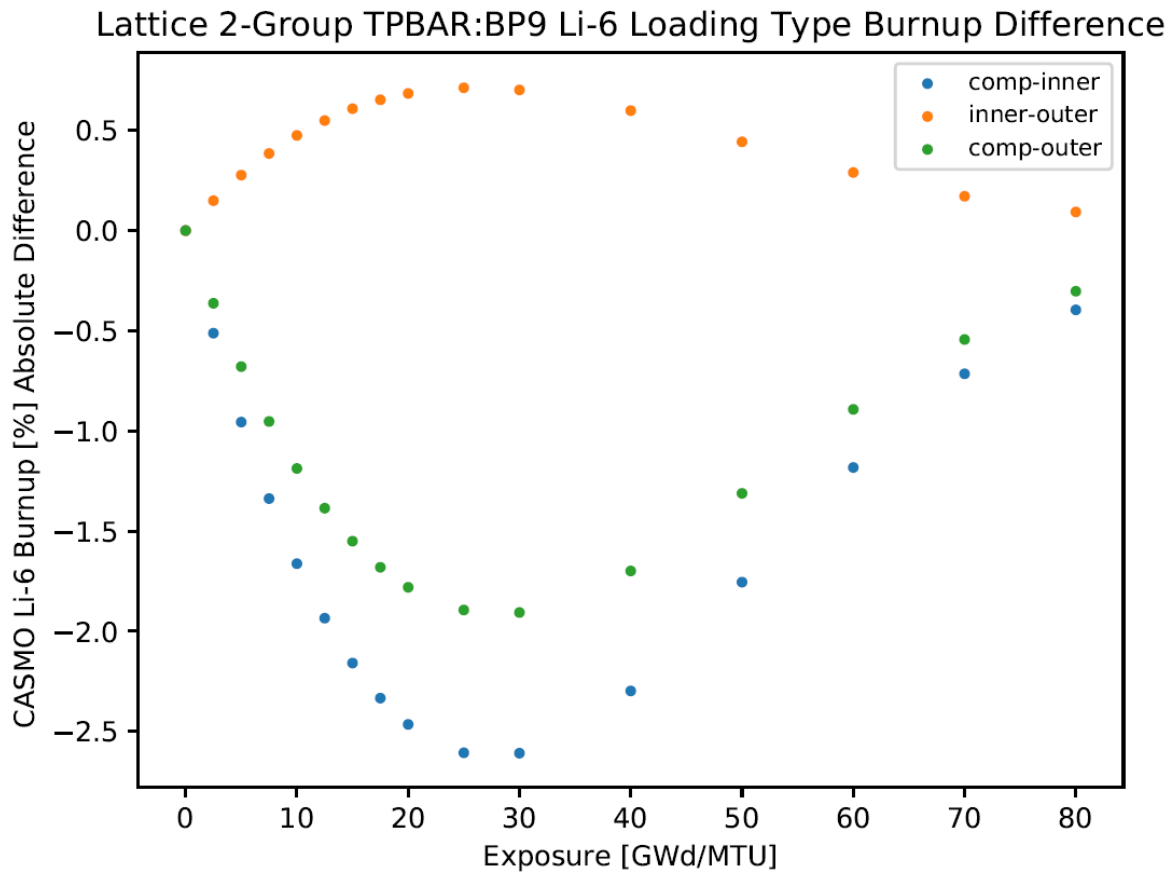


Figure 18: TPBAR Burnup Percent of Exposure for Lithium Loads

## 5.6 Lattice 2-Group Tritium Production

The following Figure 19 depicts the maximum tritium production across all loading types. The outer lithium loading has the highest tritium production at 24.003 mg/in at EOC.

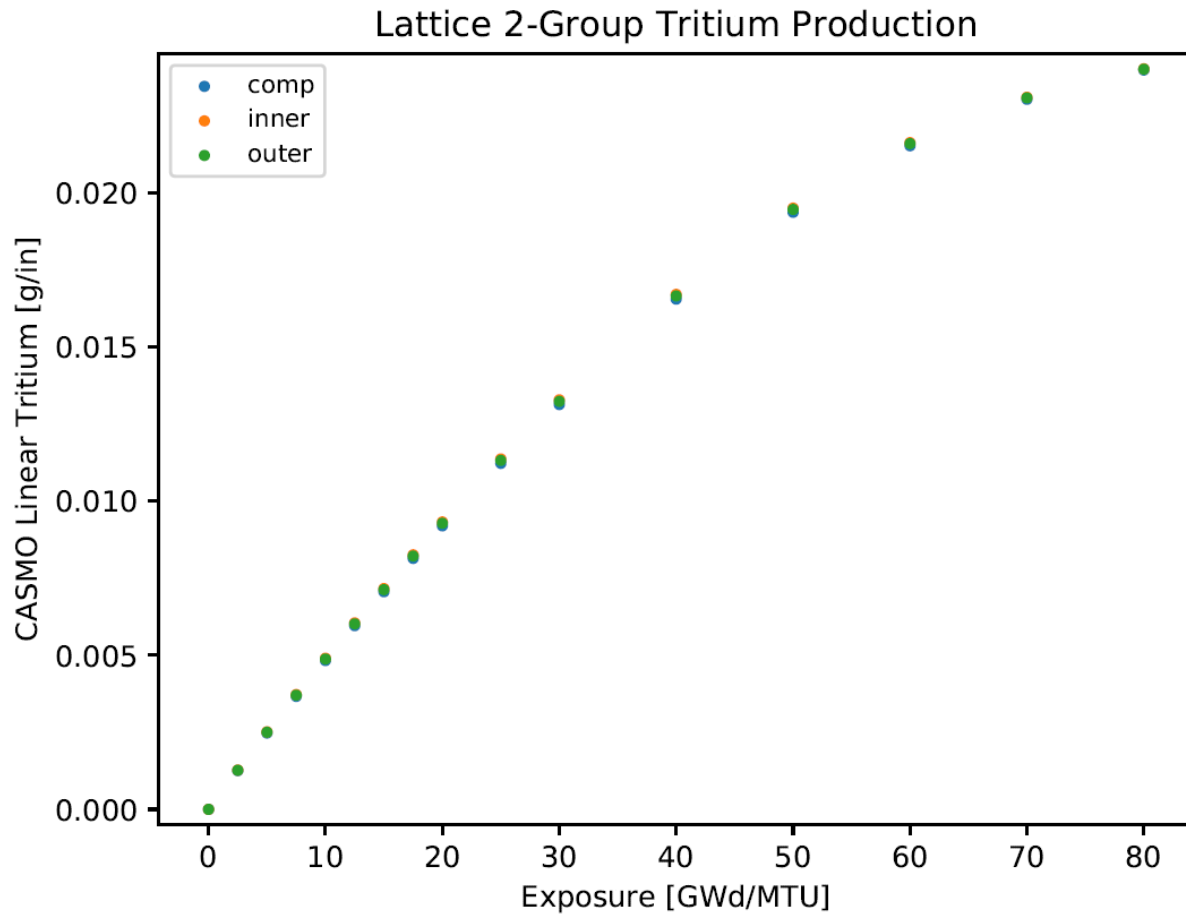


Figure 19: TPBAR Tritium Production across Lithium Loads

Table 7: Figures 19 Lattice Specifications

Maximum Tritium [mg/in]	24.0003	Exposure [GWd/MTU]	80
U-235 Enrichment [w/o]	4.80	Number of TPBAR	8
Lithium Loading [mg/in]	50	Number of IFBA	48

## 5.7 Lattice 2-Group Tritium Delta

The following Figure 20 depicts the highest tritium production deltas between loading types. The greatest difference in Tritium production is between the standard and the inner-milled pellet.

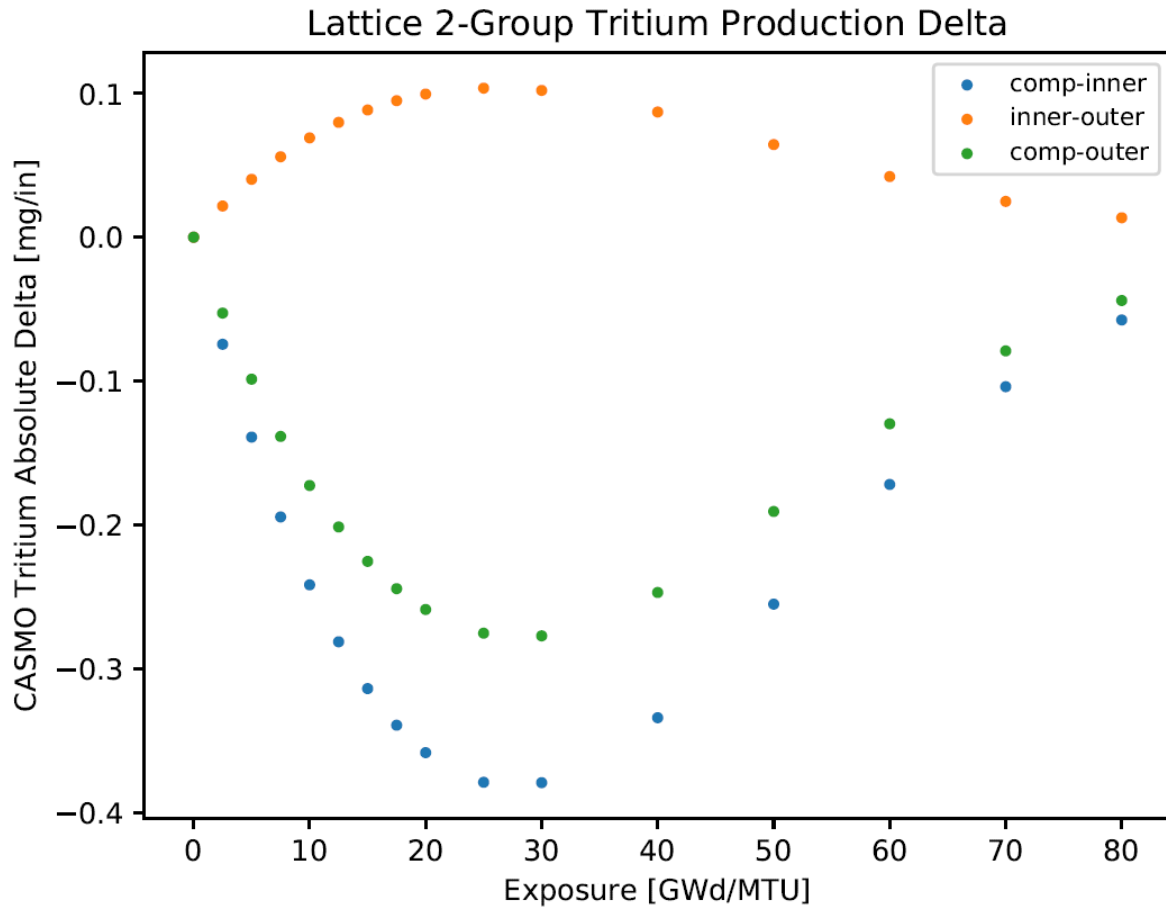


Figure 20: TPBAR Tritium Production Deltas across Lithium Loads

Table 8: Figures 20 Lattice Specifications

Maximum Tritium [mg/in]	.3791	Exposure [GWd/MTU]	80
U-235 Enrichment [w/o]	4.80	Number of TPBAR	8
Lithium Loading [mg/in]	29	Number of IFBA	0



## 5.8 CASMO5 Burnable Poison Modelling Decisions and Effects

The following plot demonstrates the CASMO5 effect of a smeared TPBAR population versus a non-smeared TPBAR, which can be illustrated in the lithium burnup absolute difference between the burnable poisons labelled as BP10 for the stationary TPBARs and BP9 for the single, potentially withdrawn TPBAR. Note that the average difference between BP9 and BP10 burnups is .0965 %, while the maximum absolute difference is 1.0174 %. This is due to the smearing of stationary TPBAR number densities, and an explicit abundance for the single, moveable BP10 TPBAR.

The impact of smearing on is greatest on the normal pellets, and smallest on the outer-milled pellets.

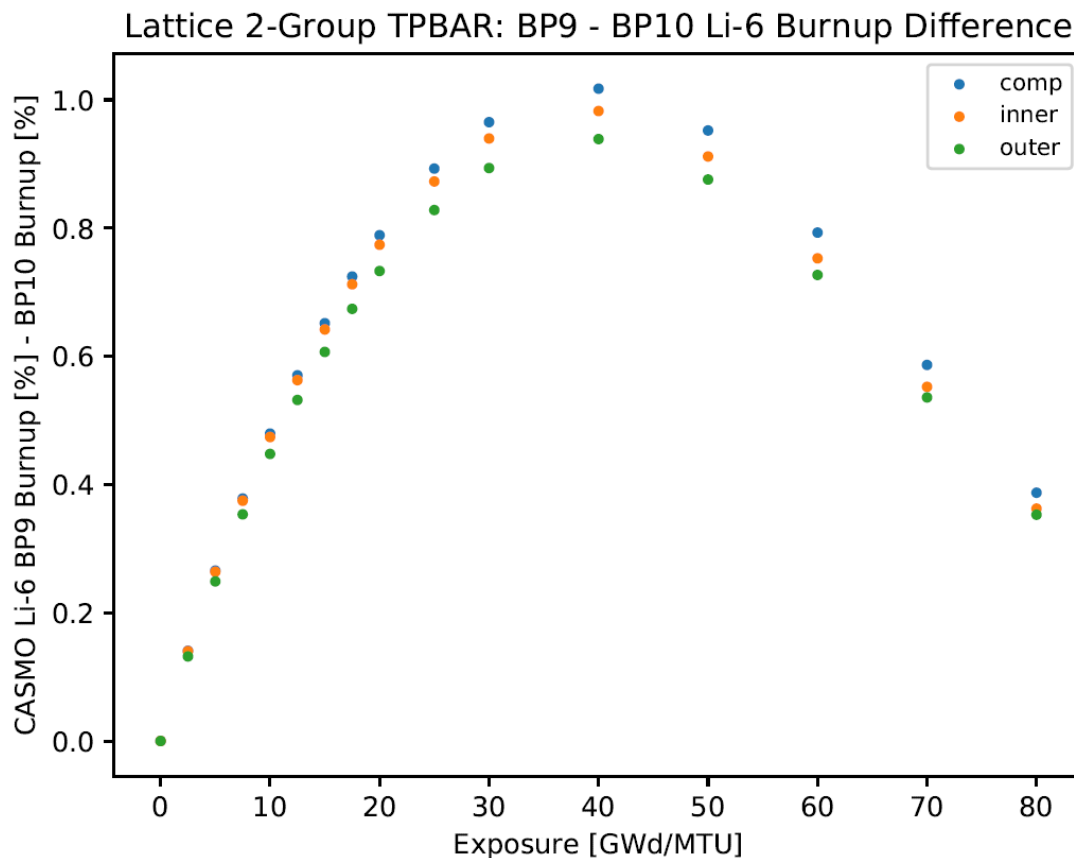


Figure 21: TPBAR ‘BP’ Specifier and Smearing Effect on Burnup Percent

Table 9: Figure 21 Lattice Specifications

Max Burnup Delta [%]	1.0174, comp	Exposure [GWd/MTU]	40
U-235 Enrichment [w/o]	4.80	Number of TPBAR	16
Lithium Loading [mg/in]	50	Number of IFBA	200

## 6.0 Conclusions

Milling a high linearly loaded Lithium Aluminate pellet's inner or outer radii to the linear loading of a standard pellet does not result in significant differences in the neutronic performance of a TPBAR at HFP, HZP or CZP across a wide range of fuel weight percent, lithium loadings, and TPBAR/IFBA lattice geometries. This offers a comparable solution for achieving a desired lithium loading by milling pellets in addition to previously used methods of manufacturing pellets to the desired loading.

The maximum TPBAR rodworth is 900 pcm, the maximum absolute rodworth delta is 127 pcm between standard pellet and an outer-radii milled pellet, and the maximum absolute delta in normalized pin power RMS is .0007. Lithium-6 burnup allows for a Tritium-produced calculation versus exposure, for which the inner-radii-milled pellet performed better than the standard pellet by producing 2.504% more tritium at 25 GWd/MTU.

Further work includes incorporating milled-pellet, lithium-loaded TPBAR models into Simulate5 and comparing Watts Bar Unit 1 Cycle performances as a function of lithium loading mechanism. This can be done to verify negligible differences in lattice performance in a broader full-core operations environment. Isolating lattices in an infinite array tends to exaggerate TPBAR worth differences between lithium loads, and so one can predict even smaller differences between milled pellets and standard pellets in a full-core simulation.

## 7.0 References

- [1] Burns, Love, Thornhill (2012, February). *Description of the Tritium-Producing Burnable Absorber Rod for the Commercial Light Water Reactor*. TTQP-1-015, Revisions 19
- [2] Godfrey, A.T. (2014, August). *VERA Core Physics Benchmark Progression Problem Specifications*. CASL-U-2012-0131-004

# **Pacific Northwest National Laboratory**

902 Battelle Boulevard  
P.O. Box 999  
Richland, WA 99354  
1-888-375-PNNL (7665)

***[www.pnnl.gov](http://www.pnnl.gov)***